Improved GWO algorithm for the determination of the critical wrinkle length of graphene

Laila Taourirte, Nour Eddine Alaa, and Hamza Khalfi

Abstract. Graphene, one of the most important discoveries in the field of materials, is an interesting two-dimensional flexible membrane which has been highly studied by physicians in the last decade as it has shown tremendous utility in fundamental studies, industrial and electronic applications, ranging from nanoelectronics to biology, thanks to its notable electronic, mechanical and chemical properties. Graphene in its natural state is non-flat and tends to crumple. The wrinkles are usually considered to be a result of stretching and bending forces, and are viewed as local minimizers of a suitable elastic energy.
In this paper we focus on the study of the wrinkling shape of graphene. A detailed geometric model provided by Yamamoto et al. [15] describing the shape of the wrinkles in terms of a deflection profile, is numerically analysed. The Euler Lagrange equation associated to this problem is formulated in the context of a constrained optimization problem and numerical simulations are carried out to compute the optimal profile using the Grey Wolf Optimizer (GWO), leading to good results in comparison with the ones found in the litterature.

2010 Mathematics Subject Classification. Primary 65K10; Secondary 65M60; 90C59.
Key words and phrases. Graphene, Wrinkle, Deflection, Euler-Lagrange, Optimisation, Grey Wolf Optimizer, Finit elements.

1. Introduction

Graphene is a two-dimensional material consisting of a one-atom thick, closely packed hexagonal carbon layer as seen in figure (1) [11]. In spite of its theorization
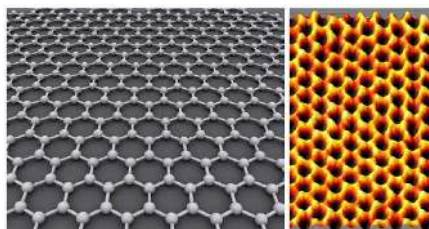

Figure 1. The ideal crystalline structure of graphene is a hexagonal grid (right) and a Scanning probe microscopy image of graphene (left).

which took place as early as 1947 by Philip R. Wallace, it was not until 2004 that Andre Geim, of the physics department of Manchester University, who received for

This paper has been presented at the Conference MOCASIM, Marrakesh, 26-27 November 2018.

this, with Konstantin Novoselov, the Nobel prize of physics in 2010, could synthesize it. This extremely thin and flexible membrane has shown tremendous utility in fundamental studies, industrial and electronic applications, ranging from nanoelectronics to biology, thanks to its notable electronic, mechanical and chemical properties, [17]. Furthermore, graphene has opened new possibilities for the storage of more lithium ions which leads to the increase of the battery's capacity [4].

It is undeniable that thin membranes strongly react to external forces and complex geometrical constraints. This phenomenon is quite natural and is exactly what happens with human skin, plant leaves and even tissues. As graphene is among the thinnest and most rigid known membranes, and because of its extremely low bending rigidity, it often tends to wrinkle [4]. During chemical vapor deposition, the graphene layers are deposited in large areas. It has been observed experimentally that these layers undergo wrinkling which causes wrinkles of several nanoparticles in amplitude, this being due to the thermal expansion between the substrate and the graphene layer. The origin of these instabilities is not yet fully understood, however, the wrinkles are usually considered to be a result of compressive stresses or stretching and bending forces. We refer the reader to [16] for detailed physical study.

In particular, the wrinkling formation in graphene has been highly studied by physicians in the last decade, as it modifies the two-dimensional structure from total planarity to wavy sheet, which can have a remarkable effect on the physical properties of graphene, such as carrier mobility, thermal conductivity, optical transmittance and wettability [11]. This deformation also affects the electronic properties of graphene, this can easily be noticed when it is bent to a certain curvature, a band gap is generated and that locally curved portion is semiconducting while the flat graphene is highly conductive [17].

Since the morphology of graphene strongly influences its physical properties, random wrinkling formation leads to unpredictable graphene properties [16]. This random change must be avoided in nanoelectronic devices in which precise control is key. For this purpose, theoretical models need to be built in order to predict graphene's response to different kinds of deformations mainly stretching and bending forces. Yamamoto et al. provided a report on experimental observations of the formation of wrinkles in a graphene layer supported on $Si0_2$ substrates with randomly placed topographic perturbations produced by $Si0_2$ nanoparticles with a dispersion density ρ_{np}, [16]. This study showed that ρ_{np} has a direct effect on the wrinkling of graphene ([15]). More precisely, at first, graphene adheres conformally to the substrate ([6], [2] and [5]) and as the nanoparticle's density increases, the wrinkles connecting the protrusions proliferate, and finally a wrinkle network spans the sample. These observations indicate the presence of a critical distance χ_c between nanoparticles, at which a transition between wrinkling and delamination occurs.

Yamamoto et al. have provided a continuum elastic model seen below in figure (2) for a graphene mono-layer deposited on a silica substrate decorated with silica nanoparticles. They presumed that each formed wrinkle between two nano-particles with diameter d separated by a distance χ, follows a Caternary-like profile. The wrinkle profile is then parametrised by a deflection $\zeta(x)$ and a maximum deflection $\zeta_0 = \zeta(0)$, $0 < \zeta_0 \leq d$. Based on these hypothesis, a one dimensional energy model has been derived stating that the actual wrinkle profile is the minimum of an energy obtained by summing both bending and stretching energies. Yamamoto and co-authors claim

that this minimum has an exact expression given by:

$$\zeta(x) = \left(\frac{27\varepsilon_2}{4\varepsilon_1}\right)^{\frac{1}{6}} \left(\frac{\chi}{2} - |x|\right)^{\frac{2}{3}}, \tag{1}$$

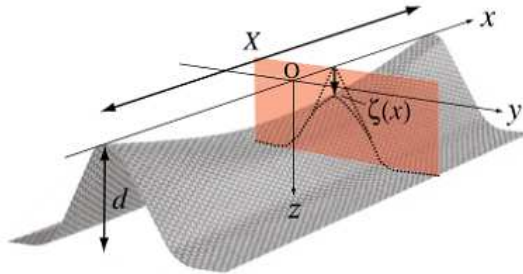where ε_i for $i = 1, 2$ are physical constants.

FIGURE 2. Deformation of graphene membrane between two nanoparticles with diameters d.

From this solution, many characteristics were deduced, such as the critical length χ_c of the wrinkle below which wrinkling is induced, and the pseudo-magnetic field created in the middle of the wrinkle which is of order 10 T for $\chi = 100$nm [15]. However the given solution suffers from slope discontinuity at $x = 0$, as mentioned by Yamamoto et al., which means it may not follow a Catenary-like profile, and the expression of this proposed minimizer could be incorrect and may imply incorrect approximations of the characteristics of the wrinkling.

Furthermore, it is not verified if this singular solution is the minimizer of the energy, nor that the associated ridge length is the critical distance between the two nanoparticles, knowing that this latter is in rough agreement with the observed maximum wrinkle length of approximately 200nm.

In order to improve this result, Guedda et al. presented a mathematical study of the same problem based on the phase-plane analysis, and identified a C^1-smooth minimizer deflection of the elastic energy, in terms of the inverse of an incomplete normalized beta function which kind of corrects the singularity from which Yamamoto's solution suffers. Using this smooth deflection, the critical wrinkle length improved however still underestimates the observed maximum wrinkle ([4]).

Zhu and Li presented a systematic molecular dynamics study of the wrinkling of graphene put on a silica substrate, and the critical wrinkle length is determined as a second degree polynomial which depends only on the nanoparticle's size d:

$$\chi_c = 2.64d^2 + 0.96d + 9.2. \tag{2}$$

However, this solution might overestimate the critical distance as one can see later [17].

Our initial aim in this paper is not to introduce another physical study of the wrinkling of graphene. Rather, an effort is made to provide a numerical algorithm that determines the critical ridge length below which wrinkling is induced, and which can be used in a more general context. The algorithm we'll be using is the Grey

Wolf Optimizer (GWO) which is a swarm-based meta-heuristic based on the social leadership and hunting behavior of grey wolves in nature (Canis Lupus), mathematically modeled by Mirjalili et al. in [9]. The obtained results show that the proposed approach provides us with a good wrinkle length in comparison with what's found in previous works.

Our paper is organised as follows: in the next section, we present in details the physical model on which we'll be basing our numerical analysis. The associated Euler-Lagrange equation is presented. The third section is dedicated to the numerical simulation using the classical method that turns out to be very hard to tackle, which will be our motivation behind using the GWO algorithm that will be described in the first subsection of the fourth section and implemented in the second one. Finally, we draw a conclusion from the showcased results.

2. Formulation of the physical problem of the wrinkled graphene in terms of optimization

The model on which we will base our numerical analysis on is the one derived by Yamamoto et al., depicted in figure (3).
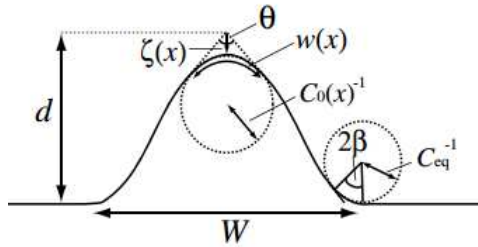

FIGURE 3. The wrinkle profile along the transverse direction.

In the deformed region, or the x projection of the wrinkling region ($i.e. |x| < \frac{x}{2}$), the elastic energy is expressed as a summation of the stretching energy given by:

$$E_s = \frac{\text{E}_{2\text{D}}}{2} \int_{|x|<\frac{x}{2}} \omega(x)\varepsilon_x^2 dx$$

and the bending energy given by:

$$E_b = \frac{\text{k}}{2} \int_{|x|<\frac{x}{2}} \omega(x)C_0^2(x)dx,$$

where $\text{E}_{2\text{D}} \approx 2.12 \times 10^3 \ ev/nm^2$ is the tensile rigidity [7], $\text{k} \approx 1 \ ev$ is the bending rigidity [3], ω is the width of the deformed region, $\varepsilon_x \approx \frac{(\partial_x \zeta)^2}{2}$ is the stretching strain which is supposed to be irrelevant in the y-direction, C_0 is the curvature that describes the profile of the ridge along the transverse direction, and θ is the dihedral angle which is assumed to be independant of x as validated in [8].

We can prove from the model that :

$$\omega(x) = (\pi - \theta)\, C_0^{-1}(x)$$

and

$$C_0 = \zeta(x) \left[\frac{1}{\sin(\frac{\theta}{2})} - 1 \right]^{-1}$$

As a consequence, the elastic energy is expressed as follows:

$$\mathcal{F}(\zeta) = \varepsilon_1(\theta) \int_{|x| < \frac{\chi}{2}} \zeta \left(\partial_x \zeta \right)^4 dx + \varepsilon_2(\theta) \int_{|x| < \frac{\chi}{2}} \zeta^{-1} dx,$$

where

$$\varepsilon_1(\theta) = \frac{E_{2D}}{8} (\pi - \theta) \left[\frac{1}{\sin(\frac{\theta}{2})} - 1 \right]^{-1},$$

$$\varepsilon_2(\theta) = \frac{k}{2} (\pi - \theta) \left[\frac{1}{\sin(\frac{\theta}{2})} - 1 \right].$$

The adhesion energy to the substrate is given by:

$$E_a = 2\Gamma\chi \, d \, \tan\left(\frac{\theta}{2}\right),$$

where Γ is the graphene-SiO_2 adhesion energy per area.

The adhesion and the bending energies at the foot of the wrinkle denoted by $E_{a'}$ and $E_{b'}$ respectively turn out to be negligible [15]. Finally, the expression of the total energy is given by the sum of all these energies :

$$E(\zeta) = \mathcal{F}(\zeta) + E_a + E_{a'} + E_{b'}.$$

The goal is to obtain the pair (ζ_c, χ_c) corresponding to a local minimizer of the total energy under the boundary conditions $\zeta(\frac{\pm\chi}{2}) = 0$, and the maximal length of the wrinkle. Indeed, at first, they assume that θ varies arbitrarily. This is physically not correct since the graphene profile must have a critical angle that minimizes the total energy. Hence, to determine this angle, the authors derive a scaling law for the critical nanoparticle separation. We refer the reader to the appendixes of [4] and [15] for detailed analysis.

As mentioned in the introduction, the authors in [15] claim that there exists an exact expression minimizing the total energy given by (1), which leads to a critical wrinkle length given by:

$$\chi_c = d^{\frac{3}{2}} \left(\frac{64E_{2D}}{27k} \right)^{\frac{1}{4}} \left[\frac{1}{\sin(\frac{\theta}{2})} - 1 \right]^{-\frac{1}{2}}. \tag{3}$$

However the given solution suffers from slope discontinuity at $x = 0$, which means it doesn't necessarily follow a Catenary-like profile and then the expression (3) may be not correct.

On the other hand, in [4], the authors gave an estimation of the critical wrinkle length that gave closer results to the observed length:

$$\chi_c = d^{\frac{3}{2}} \left(\frac{3E_{2D}}{4k} \right)^{\frac{1}{4}} \left[\frac{1}{\sin(\frac{\theta}{2})} - 1 \right]^{-\frac{1}{2}} \bar{\chi}, \tag{4}$$

$\bar{\chi}$ is the inverse of an incomplete normalized beta function that corrects the singularity from which Yamamoto's solution suffers. Using this result led to better results,

however still not sufficiently close to the observed length. Furthermore, injecting this critical wrinkle length in the expression of the total energy as a function of θ, they obtained an expression that makes the minimization problem impossible to solve analytically. Hence, they only evaluated the critical angle in two regimes (bending-dominated regime and stretching-dominated regime). For intermediate regimes, θ_c can only be determined numerically.

In this paper we hope to provide a numerical investigation that allows us to identify the critical wrinkle length associated to the critical dihedral angle θ_c that minimizes the energy. First of all, we set a well posed mathematical formulation by adding a set of constraints. The problem is to minimize the energy $\mathcal{J}$ defined by :

$$
\begin{cases}
\mathcal{J}(\zeta) = \varepsilon_1(\theta) \int_{|x| < \frac{\chi}{2}} \zeta \left(\zeta_x \right)^4 + \varepsilon_2(\theta) \int_{|x| < \frac{\chi}{2}} \zeta^{-1} + 2\Gamma\chi d \tan\left(\frac{\theta}{2} \right), \\[2ex]
\text{subject to } \zeta(\pm\tfrac{\chi}{2}) = 0.
\end{cases}
\tag{5}
$$

The functional defined above can be rewritten using a change of variable $v = \zeta^{\frac{5}{4}}$:

$$
\begin{cases}
\mathcal{J}(v) = \left(\tfrac{4}{5} \right)^4 \varepsilon_1(\theta) \int_{|x| < \frac{\chi}{2}} (v_x)^4 + \varepsilon_2(\theta) \int_{|x| < \frac{\chi}{2}} v^{-\frac{4}{5}} + 2\Gamma\chi d \tan\left(\frac{\theta}{2} \right), \\[2ex]
\text{subject to } v(\pm\tfrac{\chi}{2}) = 0.
\end{cases}
\tag{6}
$$

Theorem 2.1. *The functional $\mathcal{J}$ admits a local minimum v in K that satisfies the associated Euler-lagrange equation:*

$$
\begin{cases}
-\varepsilon_1(\theta)(v_x^3)_x = \frac{5^3}{4^4}\varepsilon_2(\theta)v^{\frac{-9}{5}} \qquad \mathcal{D}'(]-\tfrac{\chi}{2}, \tfrac{\chi}{2}[) \\
\qquad\qquad v(\pm\tfrac{\chi}{2}) = 0,
\end{cases}
\tag{7}
$$

where:

$$
K = \left\{ v \in W_{loc}^{1,4}(]-\tfrac{\chi}{2}, \tfrac{\chi}{2}[) / v^{-\frac{4}{5}} \in L^1(]-\tfrac{\chi}{2}, \tfrac{\chi}{2}[) \text{ and } v^{\frac{6}{5}} \in W_0^{1,4}(]-\tfrac{\chi}{2}, \tfrac{\chi}{2}[) \right\}.
$$

Proof. see [12]. □

3. Classical optimization approaches and algorithms

As mentioned in [15], a wrinkle is geometrically suppressed if $v(0) >= d^{5/4}$, hence the maximum length of a wrinkle will be determined under the condition $v(0) = d^{5/4}$. Note that $v(0)$ is in fact $v_{\chi,\theta}(0)$ denoted like that for simplification. We express the optimization problem as follows:

$$
\begin{cases}
Minimize \quad \mathcal{F}(\chi, \theta) = | v(0) - d^{5/4} |^2, \\
\text{where } v \text{ is the unique solution to (7).}
\end{cases}
\tag{8}
$$

The Lagrangian is then given by:

$$
\mathcal{L}(v, \phi, \theta, \chi) = \mathcal{F}(\chi, \theta) + \varepsilon_1(\theta) \int_{|x| < \frac{\chi}{2}} v_x^3 \phi_x \, dx - \frac{5^3}{4^4}\varepsilon_2(\theta) \int_{|x| < \frac{\chi}{2}} v^{\frac{-9}{5}} \phi \, dx.
$$

Using the rapid derivation [1], we obtain:

(i)- $-\varepsilon_1(\theta)((v_x)^3)_x = \frac{5^3}{4^4}\varepsilon_2(\theta) \, v^{\frac{-9}{5}}$;

(ii)- $-\frac{4^4}{5^3}3\varepsilon_1(\theta)(v_x^2\phi_x)_x + \frac{9}{5}\varepsilon_2(\theta)v^{\frac{-14}{5}}\phi = -2(v(0) - d^{5/4})\,\delta_0$, where δ_0 is a dirac mass at the origin;

(iii)- $\mathcal{F}'(\theta) = -\frac{\partial}{\partial\theta}\varepsilon_1(\theta)\int_{|x|<\frac{\chi}{2}} v_x^3\phi_x + \frac{5^3}{4^4}\frac{\partial}{\partial\theta}\varepsilon_2(\theta)\int_{|x|<\frac{\chi}{2}} v^{\frac{-9}{5}}\phi$;

(iiii)- $\mathcal{F}'(\chi) = -\frac{1}{2}\frac{4^4}{5^3}\varepsilon_1(\theta)[(v_x(\frac{\chi}{2}))^3\phi_x(\frac{\chi}{2}) + (v_x(\frac{-\chi}{2}))^3\phi_x(\frac{-\chi}{2})]$.

The first equation can be solved using the regularized problem as one can see later on, but the second one is very hard to tackle if not impossible due to the degeneracy of its first term, which is our motivation behind using meta-heuristics. The main steps of this classical method using the finite elements are described in Algorithm 1 , where V_h is the P^1 finite element space, χ the distance between the two nanoparticles of diameters d, ϵ the tolerance, α, β and η are the steps of the gradient descent.

Algorithm 1 Steps of the classical method

---

while $|v^n - v^{n-1}| \geq \varepsilon$ **do**

  • Solve for w^n the equation below $\forall\psi \in V_h$

$$\int_{|x|<\frac{\chi}{2}} w_x^n\psi_x = \int_{|x|<\frac{\chi}{2}} \varepsilon_1(\theta)((v_x^n)^3)\psi_x - \frac{5^3}{4^4}\varepsilon_2(\theta)(v^n)^{\frac{-9}{5}}\psi$$

  • Update $v^n \leftarrow v^n - \alpha\, w^n$

end while

• Solve the equation below $\forall h \in V_h$

$$\frac{4^4}{5^3}3\varepsilon_1(\theta)\int_{|x|<\frac{\chi}{2}} ((v_x^n)^2)\phi_x^n h_x + \frac{9}{5}\varepsilon_2(\theta)\int_{|x|<\frac{\chi}{2}} (v^n)^{\frac{-14}{5}}\phi^n h = -2(v^n(0) - d^{5/4})h(0)$$

• Solve the equation below:

$$Y^n = -\frac{\partial}{\partial\theta}\varepsilon_1(\theta)\int_{|x|<\frac{\chi}{2}} v_x^3\phi_x + \frac{5^3}{4^4}\frac{\partial}{\partial\theta}\varepsilon_2(\theta)\int_{|x|<\frac{\chi}{2}} v^{\frac{-9}{5}}\phi$$

• Update $\theta^n \leftarrow \theta^n - \eta Y^n$

• Solve the equation below:

$$Z^n = -\frac{1}{2}\frac{4^4}{5^3}\varepsilon_1(\theta)[((v_x^n)^3(\frac{\chi}{2}))\phi_x^n(\frac{\chi}{2}) + ((v_x^n)^3(\frac{-\chi}{2}))\phi_x^n(\frac{-\chi}{2})]$$

• Update $\chi^n \leftarrow \chi^n - \beta Z^n$

Indeed, unlike the classial methods, meta-heuristics have derivation-free mechanisms: the selected solution(s) to start the optimization process with are randomly chosen, which is key in meta-heuristics. Furthermore, it is not necessary to calculate the derivatives of the search spaces to find the optimum, which makes these methods very suitable for our problem although much slower than the classical methods. Due to the stochastic nature of meta-heuristics, these algorithms are excellent in avoiding local optima compared to classical optimization techniques. This makes them capable of looking for the optimum in the entire search space.

It is worth mentioning that the No Free Lunch (NFL) theorem [13], has logically proved that there is no such thing as a perfect meta-heuristic, which means it might seem that one meta-heuristic is best-suited for one problem but may show very poor efficiency on another problem, which makes this field of study highly active, as there

are always new proposed algorithms. Some of the most well-known meta-heuristics, mainly inspired by optimization processes that occur in nature, and which are used in many works where the classical methods of Newton or fixed point type are not efficient as in [6], are: Particle Swarm Optimization (PSO), Genetic Algorithm (GA), Ant Colony Optimization (ACO), Evolution Strategy, Marriage in Honey Bees optimization (MBO), Monkey search, Bee collecting Pollen Algorithm, Bird Mating optimizer, and finally the relatively recent algorithm Grey Wolf Optimizer (GWO) based on the social hierarchy of grey wolves. This latter has shown very high performance compared to the other known meta-heuristics, we refer the reader to ([9], [10]) for detailed comparisons. In the next sections, the GWO algorithm is employed to minimize our cost function $\mathcal{F}$, and its effectiveness for our problem is evaluated by comparing the results we obtain with those obtained in literature.

4. An enhanced GWO algorithm for the determination of the critical wrinkle length of graphene

4.1. Review of the GWO search algorithm. The GWO is a swarm-based meta-heuristic based on the social leadership and hunting behavior of grey wolves in nature (Canis Lupus), mathematically modeled by [9]. The population of this algorithm is divided into four populations: alpha (α), beta (β), delta (δ) and omega (ω) (see figure 4).
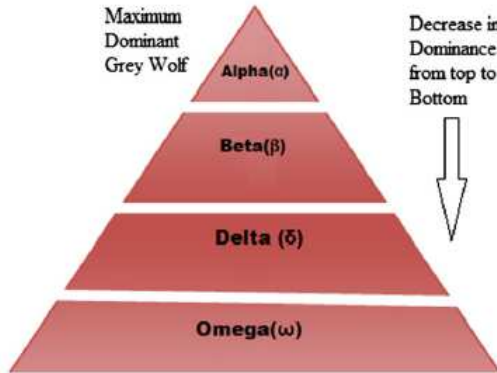

FIGURE 4. Hierarchy levels of grey wolves.

Alpha is the first category, its members are not chosen by their strength or violence but by their intelligence and decision making capacity. Beta is the second category, they help the alphas make decisions and they take their places in case one of them is absent or sick. The third category is Delta, its members are scouts, sentinels and hunters. Scouts are responsible for warning the pack in case of danger. Sentinels are responsible for the safety of the pack and hunters are the ones who help the alphas and betas during the hunt. The last category of the pack is omega. Omega wolves have to execute all the orders of the dominant wolves. The members of this class are usually the elders and the caretakers.

Alpha, beta and delta are stored as the three best solutions and the other wolves (omega) are forced to update their positions around them as follows:

$$\begin{cases} \overrightarrow{D} = |\ \overrightarrow{C}.\overrightarrow{X_p}(t) - \overrightarrow{X}(t)\ |, \\ \overrightarrow{X}(t+1) = \overrightarrow{X_p}(t) - \overrightarrow{A}.\overrightarrow{D} \end{cases}, \tag{9}$$

where t indicates the current iteration, $\overrightarrow{A} = 2a.\overrightarrow{r_1} - a$, $\overrightarrow{C} = 2.\overrightarrow{r_2}$, $\overrightarrow{X_p}$ is the position vector of the prey, $\overrightarrow{X}$ indicates the position vector of a grey wolf, a is linearly decreased from 2 to 0 for better exploration of candidate solutions which tend to diverge when $|\ \overrightarrow{A}\ | > 1$ and to converge when $|\ \overrightarrow{A}\ | < 1$ as shown in figure (5) and $\overrightarrow{r_1}$, $\overrightarrow{r_2}$ are random vectors in $[0, 1]$.

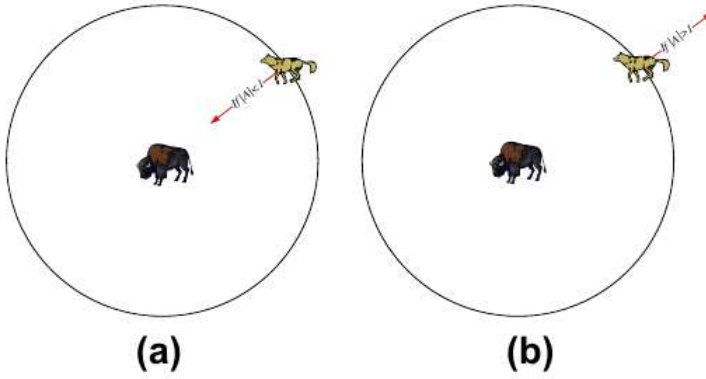FIGURE 5. Attacking prey ($|\ \overrightarrow{A}\ | < 1$) versus searching for prey ($|\ \overrightarrow{A}\ | > 1$).

Over the course of iterations, the first three fittest solutions we obtain so far are considered as α, β and δ respectively, which guide the optimization processus (the hunting) and are assumed to take the position of the optimum (the prey). The rest of the wolves are considered as ω and are required to encircle α, β and δ in order to find better results at each iteration, by following these three equations which calculate the approximate distance between the current solution and alpha, beta, and delta respectively:

$$\begin{cases} \overrightarrow{D_\alpha} = |\overrightarrow{C_1}.\overrightarrow{X_\alpha} - \overrightarrow{X}|, \\ \overrightarrow{D_\beta} = |\overrightarrow{C_1}.\overrightarrow{X_\beta} - \overrightarrow{X}|, \\ \overrightarrow{D_\delta} = |\overrightarrow{C_1}.\overrightarrow{X_\delta} - \overrightarrow{X}|. \end{cases} \tag{10}$$

$\overrightarrow{C_1}$, $\overrightarrow{C_2}$ and $\overrightarrow{C_3}$ are random vectors. $\overrightarrow{X_\alpha}$, $\overrightarrow{X_\beta}$ and $\overrightarrow{X_\delta}$ are the positions of alpha, beta and delta respectively and $\overrightarrow{X}$ is the position of the current solution.

After calculating the three distances, the final position of the solution is given by:

$$\overrightarrow{X}(t+1) = \frac{\overrightarrow{X_1} + \overrightarrow{X_2} + \overrightarrow{X_3}}{3},$$

where:

$$\begin{cases} \overrightarrow{X_1} = \overrightarrow{X_\alpha} - \overrightarrow{A_1}.(\overrightarrow{D_\alpha}), \\ \overrightarrow{X_2} = \overrightarrow{X_\beta} - \overrightarrow{A_2}.(\overrightarrow{D_\beta}), \\ \overrightarrow{X_3} = \overrightarrow{X_\delta} - \overrightarrow{A_3}.(\overrightarrow{D_\delta}), \end{cases} \tag{11}$$

$\overrightarrow{A_1}$, $\overrightarrow{A_2}$ and $\overrightarrow{A_3}$ are random vectors.

4.2. Application and implementation. Our implementation generates a population of potential solutions (wolves), they take the form of the couple (χ, θ). The fittest solution is considered as the alpha, and the second and third best solutions are considered as beta and delta respectively. The initial population is created in a random way based on the upper and lower bounds chosen for the variables χ and θ. Then we initialize the position and the score of each search agent, and we return back the search agents that go beyond the lower and upper bounds of the search space. Next, we compute the solution v that corresponds to every wolf in the population, and we deduce the minimizer of the cost function (8).

The GWO implemented in the context of this problem follows the guidelines:

• **Fitness computation**: The objective function is what is called the fitness in the algorithm. It is computed to estimate the quality of the obtained solution. In our case, in order to compute it, for each (χ, θ), we need the value of $v(0)$, where v is the solution of (7). For this purpose, we transform (7) into:

$$\begin{cases} -(|\, v_x \,|^2\, v_x)_x = -\rho_\varepsilon'(|\, v \,|) & \mathcal{D}'(] - \frac{\chi}{2}, \frac{\chi}{2} [) \\ v(\pm \frac{\chi}{2}) = 0, \end{cases} \tag{12}$$

where:

$$\rho_\varepsilon(r) = \begin{cases} -\varepsilon^{-\frac{9}{5}} r + \frac{9}{4}\varepsilon^{-\frac{4}{5}} & 0 \le r < \varepsilon \\ \frac{5}{4} r^{-\frac{4}{5}} & r \ge \varepsilon \end{cases}$$

To determine the solution v, we use the finite elements as in Algorithm 1, and we solve the equation below , for every direction ψ in the P^1 finite elements space:

$$\int_{|x| < \frac{\chi}{2}} w_x^n \psi_x \quad = \quad \int_{|x| < \frac{\chi}{2}} \varepsilon_1(\theta)((v_x^n)^3)\psi_x - \frac{5^3}{4^4}\varepsilon_2(\theta)(v^n)^{\frac{-9}{5}}\psi$$

and then we update the solution at each iteration :$v^{n+1} \leftarrow v^n - \alpha\, w^n$.
Finally, we determine $v(0)$ and calculate the cost function.

• **Selection**: We select the first three best wolves to guide the optimization (hunting) and save them as α, β and δ.

• **Update**: We update the positions of the search agents according to the positions of each category, and the parameters a, A and C. Finally, the algorithm is terminated when the end criterion is satisfied. The final generated result is the position of the alpha which is assumed to be the optimum (χ_c, θ_c), and the score of the alpha that is the value of the cost function at this optimum.

4.3. An enhanced GWO search algorithm and results. Following the previous explanation of the implementation used in our program, the main steps of the GWO applied to the optimization problem (8) are given in Algorithm 2 which we implement for 40 search agents and 80 iterations.

We investigate the critical angle θ_c in two different search spaces: the first one is the neighboring of 14° and the second one is the neighboring of 35°. Finally, for

---

Algorithm 2 Steps of the used algorithm.

1: Initialize the input parameters for GWO, i.e the number of search agents, the dimension of the problem, maximum number of iterations, lower and upper bounds of the search spaces of the variables χ and θ, and the diameter d of the silica nanoparticle.
2: Initialize Alpha, Beta and Delta Position and Score.
3: Initialize the random positions of search agents.
4: Set iteration counter $= 0$.
5: While $(t < MaxIter)$ or (stop criterion);
6: Return back the search agents that go beyond the lower and upper bounds of the search space.
7: Calculate the corresponding objective value for each wolf.
8: Select the first three best wolves and save them as α, β and δ.
9: Update the position of the rest of the population (the ω wolves) using (10) and (11).
10: Update the parameters a, A and C.
11: Go back to step (b) if the end criterion is not satisfied.
12: Return the position of α as the fittest optimum χ_c.

---

different diameters and each critical angle, we present the maximal wrinkle length χ_c obtained by the given expressions (2, 3 and 4) from the previous works on one hand, and by our algorithm on the other hand, in the tables below. Note that the mean diameter of a silica nanoparticle is 7.4 ± 2.2 nm.

TABLE 1. The critical wrinkle lengths for $d = 4.6nm$.

	χ_c (nm)	
Algorithm	$\theta_c = 15^o$	$\theta_c = 35.4432^o$
Yamamoto et al.	32.1844	54.9489
Zhu and Li	69.4784	69.4784
Guedda et al.	46.2731	79.0028
GWO	48.8693	83.4092

TABLE 2. The critical wrinkle lengths for $d = 5.2nm$.

	χ_c (nm)	
Algorithm	$\theta_c = 12^o$	$\theta_c = 35.9015^o$
Yamamoto et al.	34.1066	66.6375
Zhu and Li	85.5776	85.5776
Guedda et al.	49.0367	95.8080
GWO	52	101.40

TABLE 3. The critical wrinkle lengths for $d = 7.4nm$.

Algorithm	χ_c (nm)	
	$\theta_c = 15^o$	$\theta_c = 34.6869^o$
Yamamoto et al.	65.6684	110.4531
Zhu and Li	160.8704	160.8704
Guedda et al.	94.4147	158.8039
GWO	100	168.0948
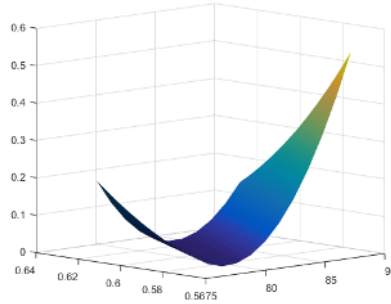
FIGURE 6. The 3d plot of the cost function vs χ and θ for $d = 4.6$ and θ in the neighborhood of 35°.
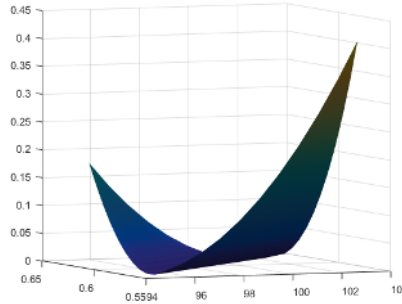
FIGURE 7. The 3d plot of the cost function vs χ and θ for $d = 5.2$ and θ in the neighborhood of 35°.

The figures (6, 7, 8) are the 3d plots of the cost function $\mathcal{F}$ in function of the critical angle θ_c and the critical length χ_c, associated to a diameter d. These plots agree well with the results prensented in the tables since the function is convex at the exact optimums (θ_c, χ_c) obtained by the GWO. Indeed, using the Grey Wolf Optimizer allowed us to numerically obtain good results in comparison with the other analytical methods, however, the observed maximum wrinkle length of 200nm is still underestimated. This is actually kind of expected since our study does not include the possibilty of the two nanoparticles that might have different diameters, as mentioned
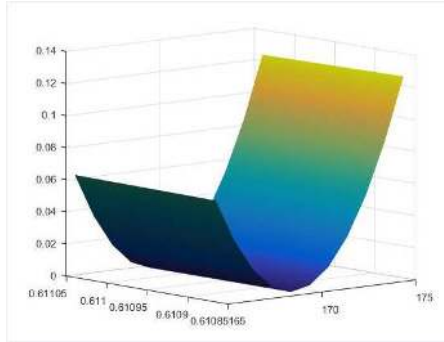
FIGURE 8. The 3d plot of the cost function vs χ and θ for $d = 7.4$ and θ in the neighborhood of 35°.

by [15], and hence the wrinkle won't have to sag in the middle, nor that the random distribution of the nanoparticles might cause that the interaction between ridges could influence the maximum wrinkle length and introduce some complicated boundary conditions, [4]. Last but not least, another possible cause behind the discrepancy between the obtained and the observed results is the other physical mechanisms such as the thermal fluctuations and the impurites that might exist on the substrate surface. This motivates our future works on the analytical and numerical aspects.

5. Conclusion

In this work, we used the Grey Wolf Optimizer algorithm to determine the critical length below which wrinkling is induced, i.e if the distance between the two nanoparticles exceeds this critical length, the caternary-like profile of the wrinkle is suppressed. Using this algorithm, we were also able to determine the critical dihedral angle θ_c that minimizes our energy for different nanoparticle's diameters. However, we haven't yet include the case of nanoparticles having different diameters in the model we based our numerical analysis on, nor the case of the random distribution of the nanoparticles by adding noise to the model, which motivate more coming works.

References

[1] J. Céa, Conception optimale ou identification de formes, calcul rapide de la dérivée directionnelle de la fonction *coût*, *ESAIM: Mathematical Modelling and Numerical Analysis* **20** (1986), no. 3, 371–402.

[2] W.G. Cullen, M. Yamamoto, K.M. Burson, J.H. Chen, C. Jang, L. Li, M.S. Fuhrer, E.D. Williams, High-fidelity conformation of graphene to SiO_2 topographic features, *Physical Review Letters* **105** (2010), no. 21, 215504.

[3] A. Fasolino, J.H. Los, M.I. Katsnelson, Intrinsic ripples in graphene, *Nature materials* **6** (2007), no. 11, 858–861.

[4] M. Guedda, N. Alaa, M. Benlahsen, Analytical results for the wrinkling of graphene on nanoparticles, *Physical Review E* **94** (2016), no. 4, 042806.

[5] M. Ishigami, J.H. Chen, W.G. Cullen, M.S. Fuhrer, E.D. Williams, Atomic structure of graphene on SiO_2, *Nano letters* **7** (2007), no. 6, 1643–1648.

[6] H. Khalfi, N.E. Alaa, M. Guedda, Period steady-state identification for a nonlinear front evolu-
     tion equation using genetic algorithms, *International Journal of Bio-Inspired Computation* **12**
     (2018), no. 3, 196–202.
[7] C. Lee, X. Wei, J.W. Kysar, J. Hone, Measurement of the elastic properties and intrinsic strength
     of monolayer graphene, *Science* **321** (2008), no. 5887, 385–388.
[8] A. Lobkovsky, S. Gentges, H. Li, D. Morse, T.A. Witten, Scaling properties of stretching ridges
     in a crumpled elastic sheet, *Science* **270** (1995), no. 5241, 1482–1485.
[9] S. Mirjalili, S.M. Mirjalili, A. Lewis, Grey wolf optimizer, *Advances in Engineering Software* **69**
     (2014), 46–61.
[10] S. Mirjalili, How effective is the Grey Wolf optimizer in training multi-layer perceptrons, *Applied
     Intelligence* **43** (2015), no. 1, 150–161.
[11] X. Shen, X. Lin, N. Yousefi, J. Jia, J.K. Kim, Wrinkling in graphene sheets and graphene oxide
     papers, *Carbon* **66** (2014), 84–92.
[12] L. Taourirte, N. Alaa, Mathematical and numerical study of a quasilinear elliptic equation with
     singular nonlinearity, *to appear*.
[13] D.H. Wolpert, W.G. Macready, No free lunch theorems for optimization, *IEEE Transactions
     on Evolutionary Computation* **1** (1997), no. 1, 67–82.
[14] J. Xue, J. Sanchez-Yamagishi, D. Bulmash, P. Jacquod, A.Deshpande, K. Watanabe, T.
     Taniguchi, P. Jarillo-Herrero, B.J. LeRoy, Scanning tunneling microscopy and spectroscopy
     of ultra-flat graphene on hexagonal boron nitride, *Nature Materials* **10** (2011), 282–285.
[15] M. Yamamoto, O. Pierre-Louis, J. Huang, M.S. Fuhrer, T.L. Einstein, W.G. Cullen, "The
     princess and the pea" at the nanoscale: wrinkling and delamination of graphene on nanoparti-
     cles, *Physical Review X* **2** (2012), no. 4, 041018.
[16] M. Yamamoto, *Two-dimensional crystals on substrates: Morphology and chemical reactivity*,
     Dissertation, Univ. of Maryland, 2013.
[17] S. Zhu, T. Li, Wrinkling instability of graphene on substrate-supported nanoparticles, *Journal
     of Applied Mechanics* **81** (2014), no. 6, 061008.

(Laila Taourirte, Nour Eddine Alaa, Hamza Khalfi) Laboratory LAMAI, Faculty of Sciences
and Techniques, University Cadi Ayyad
E-mail address: laila.taourirte@edu.uca.ma , n.alaa@uca.ac.ma, hamza.khalfi@edu.uca.ma